

# Wavelet-based Entropy Measure for Rate-Distortion Optimization in Image Coding

J. Garcia-Alvarez, H. Führ, and G. Castellanos-Domínguez

**Abstract**—A novel method for calculation of the entropy measure in wavelet space is proposed. This perceived-based entropy measure uses a Second Order Model entropy estimator, in which the occurrence of neighbors is considered in formulation. It has the intention to allow the implementation of a more suitable measure in coding processes and a relationship between the metric and the description of perceptual features. This method is used for the Rate-Distortion optimization in order to improve the bit-allocation coding algorithm, demonstrating that the wavelet-based entropy estimates a truncation step close to the target rate. The hypothesis is founded in the effect of distortion on the coefficient allocation. Because entropy measure is a close approximation of the conditional probability of image in multi-resolution space, it provides an adequate representation for the information of a *Detail* feature. A definition of Detail-based homogeneity variance criteria is used for the information quantity – wavelet representation space, in order to find the image that fits a given Quality Level criteria. Experimental results are obtained for artificial and natural databases.

**Keywords**—Entropy, Wavelet transform, Information measure, Rate distortion.

## I. INTRODUCTION

FOR the design of a coding system, an efficient balance between the estimation time and the quality of estimation of signal is a challenge, and it can be addressed by the estimation of rate values for an arbitrary quality level, in order to define which portion of signal can be transmitted for some rate restriction. Moreover, to support feature extraction techniques or another processes into the coding scheme, an adequate representation of signal in the coding process should lead to the suitable number of components that construct the portion of signal, and also it could minimize the distortion required for the rate restriction. The Rate-Distortion curve is a scheme that calculates the distortion produced by the coding process at the target rate. With this scheme, the amount of data required to transmit a portion of a image for some distortion criteria is calculated by optimization. A common optimization method uses the convex hull analysis of the Lagrangian approximation [1]. However, the optimization search is possible only after the coding process, and it does not take into account the features of the signal, i.e., when a feature of a signal is required, the extraction process requires another transformation different of the coding one. Some advantages

Sponsored by the following grants: DAAD-ALECOL 2007 Research Visitor Fellowship in RWTH Aachen University, and DIMA project "Servicio de monitoreo remoto de actividad cardiaca para el tamizaje clínico en la red de telemedicina del Departamento de Caldas".

J. Garcia-Alvarez and G. Castellanos-Domínguez are with Universidad Nacional de Colombia, S. Manizales (e-mail: jcgarciaa@bt.unal.edu.co).

H. Führ is with RWTH Aachen University.

are presented in cases where the distortion is minimized by feature estimation. Because the representation space covers the coding process for reduction of computing time and the representation of features for minimization of distortion, a better coding system for the feature can be stated, if the representation used in the coding process can be integrated. In this work, a Wavelet-based information entropy measure is proposed, in order to estimate a convenient optimized value of the Rate-Distortion curve, reducing the Lagrangian search, and to define the informativity of features with adequate representations for components in the multi-resolution space.

This work is intended to explain the advantages and challenges of the Wavelet space as an adequate representation in the case of entropy measure for Rate-Distortion curve optimization. In Section II-A we define the approximations and the occurrence calculation criteria proposed for the estimator, and the methodology for the calculation of the optimal argument for the coding scheme in Section III-C. In Section IV the results are discussed and some applications that use the method are detailed, by using some perceptual rules on Wavelet space. Conclusion is in Section V.

## II. BACKGROUND

The Shannon entropy, noted  $\mathbf{H}_1(\mathbf{X})$ , estimates for a given image matrix  $\mathbf{X}$  with elements  $x(\mathbf{m})$ ,  $\mathbf{m} \in R^2$  the occurrence probability  $P_x = P\{x(\mathbf{m}) = x\}$ , by using a first order model as follows:

$$\mathbf{H}_1(\mathbf{X}) = \sum_{x=1}^{\max x} P_x \log_2(P_x) \quad (1)$$

where the occurrences that are considered statistically independent can be calculated based on histogram, as discussed in [2]. To get a more suitable description of the image features, in cases of edge and texture processing, an analysis of the nearest neighbor  $y \in \mathbf{X}$  (see Fig. 1(a)) must be considered, specially because the feature extraction techniques are based either on the conditional probability of elements or on the joint probability [3]. By instance, the estimation of the conditional informativity can be carried out using a conditional or second order model entropy:

$$\mathbf{H}_2(\mathbf{X}) = \mathbf{H}_1(\mathbf{Y}|\mathbf{X}) = \sum_{x=1}^{\max x} P_x \sum_{y=1}^{\max y} P(y|x) \log_2 P(y|x), \quad (2)$$

being  $P(y|x) = P\{x(\mathbf{m}) = y|x(\mathbf{m} \pm 1) = x\}$  the probability of occurrences, and calculated as discussed in [3].

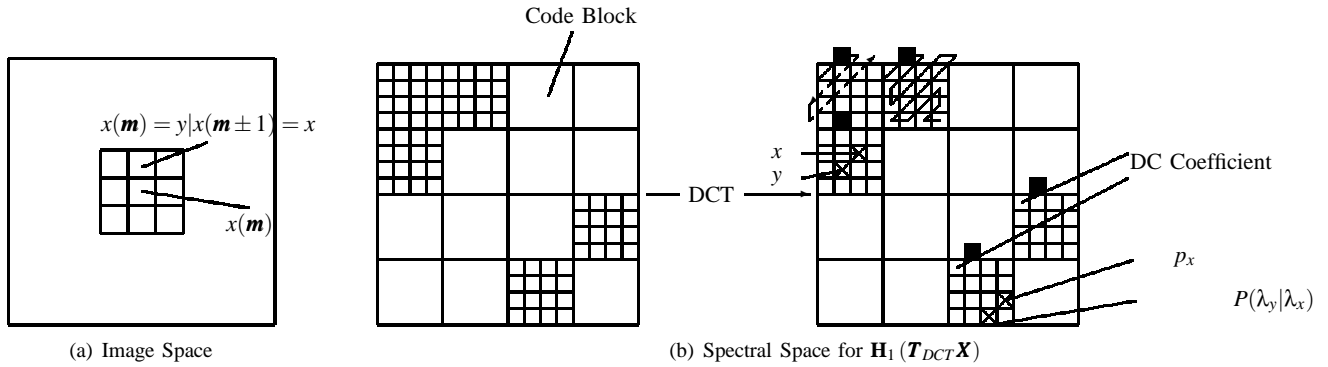


Fig. 1. Calculation of occurrence elements. In the calculation of  $\mathbf{H}_1(\mathbf{T}_{DCT}\mathbf{X})$  for a JPEG coded image, the DCT term denotes a Discrete Cosine Transform operator

### A. Estimation of Entropy using Variation Coefficient

Because of simplicity of implementation, the first order model-based entropy usually is carried out [2]. Besides, estimation of eqs. (1) and (2) needs an adequate procedure of occurrence position searching, which often is provided heuristically [3]. Computational cost depends on alphabet size. Thus, for a given  $b$ -bit alphabet that represents an image matrix of size  $M \times N$ , the number of possible elements needed to calculate the conditional or second-order entropy yields

$$\Lambda_{y|x} = \frac{(\Lambda_x \cdot \rho_y)!}{(\rho_y \cdot (\Lambda_x - 1))!}, \Lambda_x = 2^b \quad (3)$$

where  $\rho_y$  is the number of elements surrounding the pixel  $x$  whether the second order model is assumed. When the image is large, a table of huge size is required for counting occurrences (e.g.,  $\mathbf{H}_2(\mathbf{X})$  requires  $\Lambda_y$ , and  $\Lambda_{y|x}$ ). Therefore the computing time dramatically increases. So, since the occurrence calculation for a given image is computationally expensive, say  $b = 30$ , then  $\Lambda = 2^{30}$  [4], then, the translation of those measures to a multi-resolution space might be really considered to reduce the number of operations. Thus, approximations by using spectral representations are proposed in this paper, which are depicted in Fig. 1(b). Specifically, a first approximation is achieved for the entropy measure by using Quadtree decomposition (QD) based on variation coefficient criteria.

The variation coefficient values of same blocks of size  $\mathbf{B}$  and  $\mathbf{B}'$ , denoted as  $C_v$  and  $C'_v$ , respectively, can be generated by QD as shown in Fig. 2. The advantage of using those dyadic squares relies on the fact that the number of occurrences must be reduced, because only the occurrences that fit the homogeneity condition  $c_v > 1$  are considered. It locates the neighbor nearby the element, reducing the number of neighbor occurrences by 2 for each pixel. Moreover, because the size of  $\mathbf{B}$  is higher than one (size of pixel element), the number of occurrences per image also decreases, e.g., instead of computing four times the single pixel element occurrence, the 4 pixel element calculation is once accomplished. Thus, for those cases when it holds that  $C_v = v$  and  $C'_v = v'$  respective

values of  $\mathbf{H}_h$ , are estimated as follows:

$$\mathbf{H}_1(\mathbf{B}) = \sum_{v=0}^1 P_v \log_2 P_v$$

$$\mathbf{H}_2(\mathbf{B}) = \sum_{v=0}^1 P_{v'} \sum_{v'=0}^1 P(v|v') \log_2 P(v|v')$$

### B. Estimation of Entropy using Wavelet Coefficients

Further refinement of Entropy estimation is reached if the probability measuring is stated by calculation of occurrences in the spectral representation rather than in the original spatial plane [5]. Namely, the metric termed as *Wavelet Transform-based Entropy* (WTE)  $\mathbf{H}_h(\mathbf{T}_\psi\mathbf{X})$ , where  $\mathbf{T}_\psi$  is the wavelet operator, is proposed. Thus, the neighbor of the pixel is located in the same spatial position, but being at the same time in a nearby spectral position. This change in the calculation allows to define the number of occurrences  $\Lambda$  linearly (by  $j$  decomposition levels) instead of combinatorially (see eq. (3)). Algorithm 1 describes the computation of WTE, where the following  $\mathbf{H}_h$  expression for first, second and third order models, respectively, are rewritten as:

$$\mathbf{H}_1(\mathbf{T}_\psi\mathbf{X}) = \sum_{T_x} P_{T_x} \log_2 P_{T_x} \quad (4a)$$

$$\mathbf{H}_2(\mathbf{T}_\psi\mathbf{X}) = \sum_{T_x} P_{T_x} \sum_{T_y} P(T_x|T_y) \log_2 P(T_x|T_y) \quad (4b)$$

$$\mathbf{H}_3(\mathbf{T}_\psi\mathbf{X}) = \sum_{T_x} P_{T_x} \sum_{T_y} P(T_y|T_x) \times \sum_{T_z} P(T_z|T_y, T_x) \log_2 P(T_z|T_y, T_x) \quad (4c)$$

where  $P_{T_x}$  is the occurrence probability of the Wavelet coefficient  $c(j) = T_x$ ,  $c(j-1) = P_{T_y}$  the probability of occurrence of the neighbor  $T_y$ , for some decomposition scale  $j$ , and  $T_z$  is the event after  $T_y$ .

## III. EXPERIMENTAL SET-UP

### A. Validation Databases

Concrete results of estimation for proposed Wavelet-based Entropy measure are achieved for the following three considered image databases:

- *Art* - Artificially drawn images composed by 5 images shown in Fig. 4.
- *Nat* - Photography images, extracted from [6], composed by 29 photograph images. Because the images

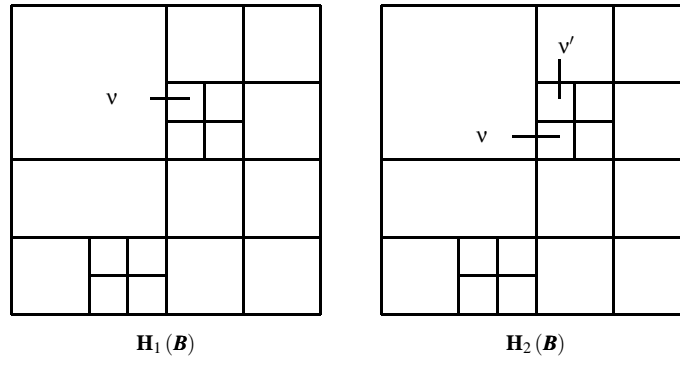


Fig. 2. Calculation of occurrence elements by Quadtree Decomposition

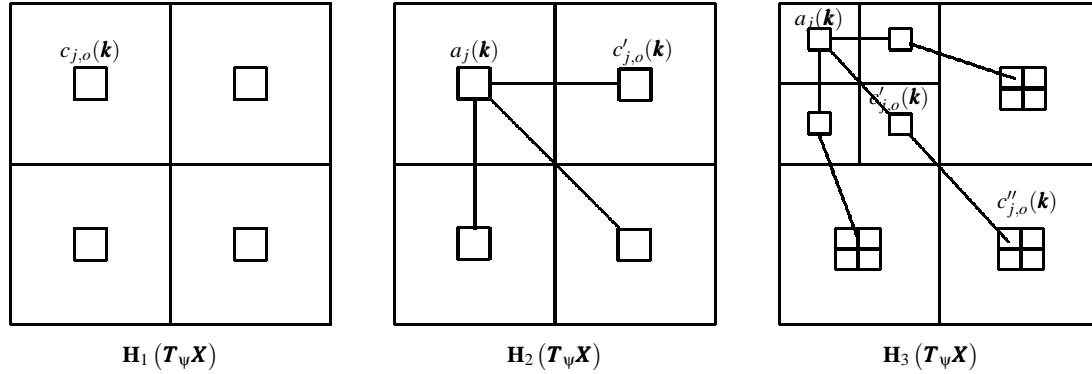


Fig. 3. Calculation of occurrence elements in Wavelet space

---

**Algorithm 1** Calculate  $WTE\{X\} = H_h(\mathbf{T}_\psi \mathbf{X})$ 


---

**Require:**  $\mathbf{c} = \mathbf{T}_\psi \mathbf{X}$  approximation coefficients  $a(\mathbf{k}) \in \mathbf{c}$ 
**Ensure:**  $\exists c'_{j,o}(\mathbf{k})$  as descendant of  $c_{j,o}(\mathbf{k})$ , so that  $c'_{j,o}(\mathbf{k}) = c_{j-1,o}(\mathbf{k})$ .

 Normalize coefficients  $\mathbf{c} = \mathbf{c} \cdot 2^{-J}$ 

 The approximation coefficients  $a(\mathbf{k}) = c_j(\mathbf{k})$  have descendants  $c'_{j,o}(\mathbf{k})$ , for  $j = 1 \dots J$  and  $o = 1, 2, 3$ .

**for all**  $\mathbf{c}$  **do**

 Calculate the counts of occurrences  $c_{j,o}(\mathbf{k}) = \mathbf{T}x$  for  $h = 1, 2, 3$ ,  $c_{j+1,o}(\mathbf{k}) = \mathbf{T}y$  for  $h = 2, 3$  and  $c_{j+2,o}(\mathbf{k}) = \mathbf{T}z$  for  $h = 3$ , by quantized beans of  $\lfloor 1/\max \mathbf{c} \rfloor$ , as shown in Fig. 3.  $\lfloor \cdot \rfloor$  denotes floor operation.

**end for**


---

are RGB, they have been converted to gray-scale. Those images contain default quality index values  $Q_0$  defined as *Differential Mean Observed Scores* (DMOS) [7]. Some examples are shown in Fig. 5.

- *ROI-Mammogram* - Mammogram image, shown in figure 6(a), with inclusion of the Region-of-Interest (ROI) enhancing process, as explained in [8].

It must be quoted that the all image sets have 8-bit resolution, in order to homogenize the quantization space for the three databases. Besides, each studied image is encoded in truncated segments  $t_i$ , where the target quality restriction  $Q_0$  can be found in some of the calculated intervals  $Q(t_i)$ . Specifically, a target quality of  $Q_0 = 85$  for the ROI enhancing,

based on a previous analysis of radiological images, is used for the *ROI-Mammogram* database. For the Rate-Distortion optimization process, the used IQ metric is proposed in [9] for the calculation of the  $t_i$ .

Testing and validation of discussed methodology, proposed for Wavelet-based entropy measure oriented to Rate-Distortion curve optimization, comprises the following two stages: i) Comparison of entropy calculated for each order  $h$ , and ii) Rate-Distortion curve optimization.

### B. Comparison of estimated entropy

Before accomplishing the optimization process, the entropy is calculated by using Equations (4a), (4b) and (4c) by using the *Art* and *Nat* data bases, in order to show their performance between natural and artificial images. Moreover, the Shannon Entropy from Equations (1) and (2) is measured to establish how long the proposed measure changes. Considered comparison is carried out according to the Algorithm 2.

### C. Rate-distortion curve optimization

Recent data coding techniques use Quality-Layer-supported structures that allows streams to be sent progressively with a high-indexed layer feature. For this structure, the *Layer-Resolution-Codeblock-Precint* (LRCP) coding scheme is used [1]. This scheme provides the sequence of estimated rates for a number  $I$  of Quality layers  $Q_i$ ,  $i = 1, \dots, I$ . The target rate  $R_i$  is calculated from the discrete number of truncation steps  $t_i$  required for displaying a given section of image  $\mathbf{X}_{m \times n}$ .

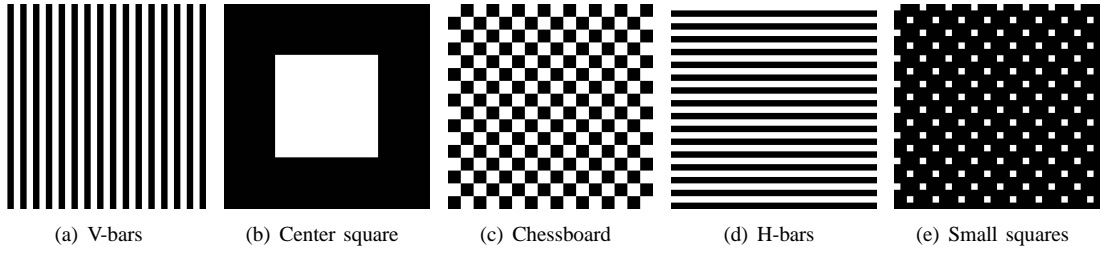
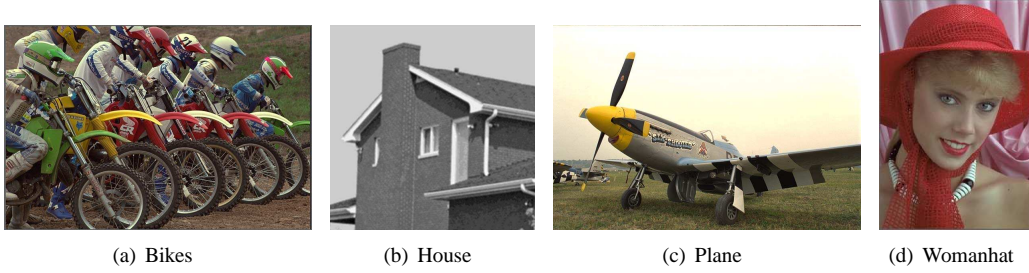
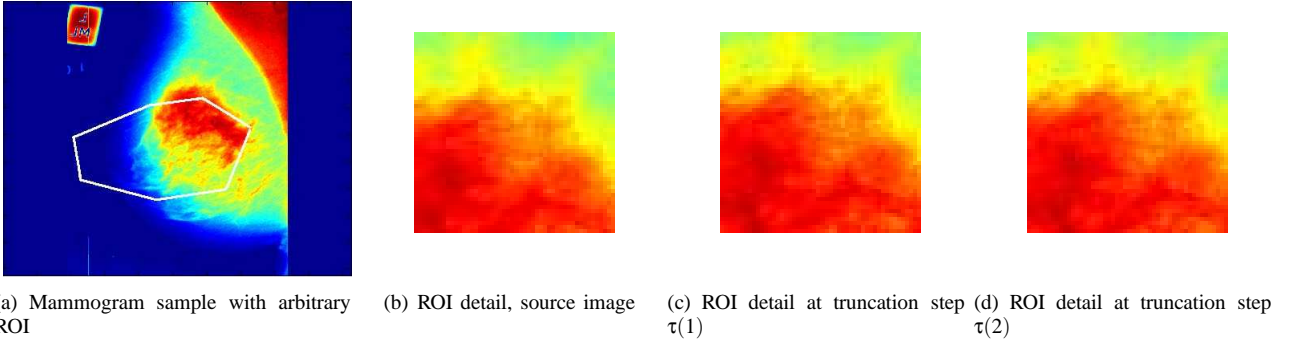
Fig. 4. Test images. Set *Art*Fig. 5. Some test images from set *Nat*

Fig. 6. Test of ROI extraction method. Type of image: 8-bit gray-scale Mammogram. Size of image: 1024x1024. Coordinates of ROI selected polygon:  $m(\text{rows}, \text{cols}) = \{(210, 507), (225, 670), (438, 743), (655, 706), (728, 471), (587, 367), (427, 387), (210, 507)\}$ . The image belongs to the mini-MIAS database of mammograms. Data selected: mdb209.pgm. See [10] for details.

---

**Algorithm 2** Comparison of  $\mathbf{H}_h$ 


---

**Require:**  $\mathbf{T}_{\Psi}\mathbf{X}$ 
**for all** Images in *Art* and *Nat* databases **do**
**for**  $h = 1, 2, 3$  **do**

    Calculate  $\mathbf{H}_h(\mathbf{T}_{\Psi}\mathbf{X})$ , by using Algorithm 1. The haar wavelet family is used.

    Calculate  $\mathbf{H}_1(\mathbf{X})$  and  $\mathbf{H}_{SLB}(\mathbf{X})$ .

**end for**
**end for**


---

Then, for a fixed  $t_i$ , there is a sequence of truncated streams  $\{\mathbf{T}_{\Psi}\mathbf{x}\}(t_i) \subseteq \{\mathbf{T}_{\Psi}\mathbf{X}\}$ , each with length  $L_{t_i}$ , that is sent at rate  $R_i$ . Under preassumption of a noiseless condition, the stream is transmitted in  $L(t_i)/R_i$  time. Each block  $\{\mathbf{T}_{\Psi}\mathbf{x}\}(t_i)$  is transmitted in a given order depending on the feature required to be displayed firstly, i.e., energy-relevant feature data should be sent at the beginning to display the estimated portion of the image. Thus, if the overall length is limited by  $L_{\max}$ ,

the rate allocation problem consists in the searching of the largest truncation point,  $\tau \in t_i$ , such that the total length of the streams matches the inequality,  $\sum_i L(\tau) \leq L_{\max}$ , and thus the set minimizes the distortion value [11]:

$$D = \sum_i D(t_i) \quad (5)$$

where  $D(t_i) = d(\mathbf{X}, \tilde{\mathbf{X}})$ , and  $\tilde{\mathbf{X}} = \mathbf{T}_{\Psi}^{-1} \cup_i \{\mathbf{T}_{\Psi}\mathbf{x}\}(t_i)$ , is the estimated image. Thus, assuming that the corresponding rate-distortion slopes  $\Delta D(t_i)/\Delta \mathbf{H}_h(\mathbf{T}_{\Psi}\mathbf{X})$  are strictly decreasing,  $\tau$  is the argument to find the suitable  $\lambda$  that fits the following optimization function [1], [12], [13].

$$\min \left\{ \left( -\sum_b \mathcal{E}\{D(\mathbf{X}, t_i^\lambda)\} \right) + \lambda \left( \sum_b L(\mathbf{X}, t_i^\lambda) \right) \right\} \quad (6)$$

where  $D(\mathbf{X}, t_i^\lambda)$  is the distortion metric associated to the image  $\mathbf{X}$ , at truncation level  $t_i$  for the stream  $\{\mathbf{T}_{\Psi}\mathbf{x}\}(t_i)$ ,  $\mathcal{E}\{\cdot\}$  stands for the expectation operator, and  $L(\mathbf{X}, t_i^\lambda)$  is the length of stream  $\{\mathbf{T}_{\Psi}\mathbf{x}\}_{t_i}$ . The hypothesis states that the entropy  $\mathbf{H}_h(\mathbf{T}_{\Psi}\mathbf{X})$  is located close to the length value  $L(\tau)$  that

corresponds to  $\tau$  so that the following expression might be minimized:

$$D(\tau) = d(\{\mathbf{T}_{\Psi^x}\}(\tau), \mathbf{T}_{\Psi}\mathbf{X}) d\left(\sum_{t_i=1}^{\tau-1} \{\mathbf{T}_{\Psi^x}\}(t_i), \mathbf{T}_{\Psi}\mathbf{X}\right)$$

The calculation of  $\tau(h)$ , discussed in [14], is described in Algorithm 3. The rate steps are calculated by using the LRCP JPEG2000 coding scheme. The Kakadu V6.0 software is used for this step. Each stream  $\{\mathbf{T}_{\Psi^x}\}(t_i)$  that is associated with an estimator of value  $L(t_i)$ , as well as a related *Quality level*,  $Q(t_i)$ , is compared with Wavelet-transformed version  $\mathbf{T}_{\Psi}\mathbf{X}$ , by using an objective metric. The distortion of the decoded image  $\mathbf{T}_{\Psi^x}^{-1} \sum_{t_i=1}^{\tau(h)} \{\mathbf{T}_{\Psi^x}\}$  at step  $\tau(h)$  is measured by the Mean Square Error (MSE).

---

**Algorithm 3** Calculate  $\tau(h)$  for RD Curve
 

---

**Require:**  $\mathbf{c} = \mathbf{T}_{\Psi}\mathbf{X}$

**for all**  $h = 1, 2, 3$  **do**

**repeat**

    Calculate  $\tilde{L}(\tau') = \mathbf{H}_h(\mathbf{T}_{\Psi}\mathbf{X})$

    By using the LRCP scheme estimated by (6),  $\alpha$  is the step calculated by the scheme for each  $R(t_i)$  by  $t_i = 1, \dots, I$  intervals.

    Calculate the candidate set  $\{\tilde{R}(t_i)\}$ :

$$\{\tilde{L}(t_i)\} = \{\tilde{L}(\tau') - \alpha, \tilde{L}(\tau'), \tilde{L}(\tau') + \alpha\}$$

    Calculate the set  $\{D(t_i)\}$  where, for some  $t_i$

$$D(t_i) = d(\{\mathbf{T}_{\Psi^x}\}(t_i), \mathbf{T}_{\Psi}\mathbf{X})$$

    Calculate the set  $\{\Delta(t_i)\}$  where, for some  $t_i$

$$\Delta(t_i) = \frac{D(t_i) - D(t_i - 1)}{L_h(t_i) - L_h(t_i - 1)}$$

**if**  $\Delta(t_i) < 0$  **then**

$\Delta_0 = \min \Delta(t_i)$

$t_i = t_{i+1}$

**end if**

**until**  $\Delta_0 < \epsilon$

$\tau(h) = \tau'$

**end for**

Calculate  $D$  for  $\tau(h)$

---

## IV. RESULTS AND DISCUSSION

### A. Comparison of estimated entropy

Even though expression (1) assumes that the occurrences are statistically independent, still considerable variations of distortion lead to a relevant modification of image density probability, validating the need for the calculation of (2), and showing that Wavelet-based information quantity is a good approximation for the conditional probability parameter. Results of this comparison, depicted in Tables I and II, show that information quantity measured at Wavelet representation space can be used to estimate the adequate truncation  $\tau$ .

Moreover, estimation of  $\mathbf{H}_2(\mathbf{T}_{\Psi}\mathbf{X})$  is sensible to transitions between neighbor occurrences, and it could indicate where a

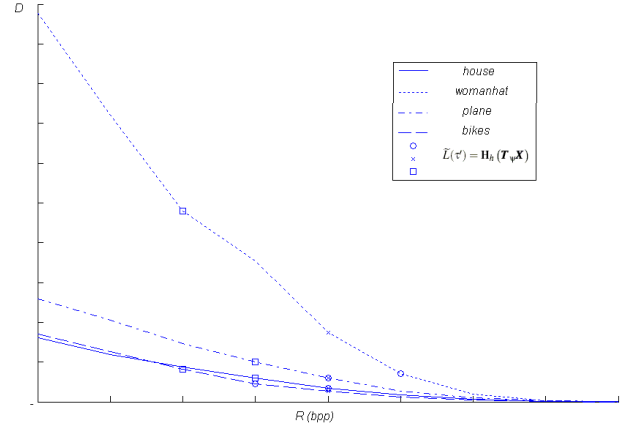


Fig. 7. Rate Distortion curve for the images in database *Art*, with the  $\tau(h)$  values. Circles: Distortion calculated at  $\tau(1)$ . Crosses: Distortion calculated at  $\tau(2)$ . Squares: distortion calculated at  $\tau(3)$ .

*detail* set for a feature  $k_c$  accomplishes the variance criteria, because this measure can be separated by orientation, i.e., for a given index  $\{j, k, o\}$ , the event  $\{\mathbf{c} : c_{j,k,o} \in \mathbf{T}_x\}$  can be statistically independent of  $\{\mathbf{c} : c_{j,k,o \pm 1} \in \mathbf{T}_y\}$ . Thus, the definition of *detail* set, as function of a directional component of  $\mathbf{c}_{k_c}$ , is useful for feature analysis. As result of this work, one can state that the features are not necessary to be represented in a space different from the used for the coding scheme, and thus the metric used for the Wavelet space gives information about the effect of directions, regarded as a feature of relevant information for *detail* set. Finally, for the test databases *Art* and *Nat*, the following inequalities take place

- 1)  $\mathbf{H}_h(\mathbf{T}_{\Psi}\mathbf{X}) < \mathbf{H}_1(\mathbf{X})$
- 2)  $\mathbf{H}_h(\mathbf{T}_{\Psi}\mathbf{X}) < \mathbf{H}_{h-1}(\mathbf{T}_{\Psi}\mathbf{X})$
- 3)  $\mathbf{H}_h(\mathbf{T}_{\Psi}\mathbf{X})|_j < \mathbf{H}_h(\mathbf{T}_{\Psi}\mathbf{X})|_{j+1}$

After comparison of outcomes of Tables I and II, it can be seen that only in case of  $\mathbf{H}_1(\mathbf{T}_{\Psi}\mathbf{X})$  the variation of entropy regarding to  $j$  should be accepted as remarkable. Therefore, testing is afterward provided for the fixed value  $j = 4$ .

### B. Rate-Distortion optimization

Fig. 6(c) and 6(d) show a detail of the ROI boundary when the image is coding by using  $\mathbf{H}_h(\mathbf{T}_{\Psi}\mathbf{X})$  as target rate. In comparison to 6(b), when the coding of the image by using the  $\tau$  estimated from  $\mathbf{H}_2(\mathbf{T}_{\Psi}\mathbf{X})$ , there is an improvement in the preservation of the ROI. Besides, since the result in 6(d) turns to be similar to 6(c), the analysis based on the third order model estimator is assumed not to be further required. Fig. 7 and 8 evidences that  $\tau(h)$  decreases as  $h$  grows in the Rate-Distortion curve and the localization of  $\tau(h)$  is very close to the  $\mathbf{H}_h(\mathbf{T}_{\Psi}\mathbf{X})$  value. This result also points out that the entropy takes advantage of the redundancy during its calculation.

Because images can be represented by spatial-spectra spaces, a image feature, e.g., contours, edges and objects, can be classified in some component in order to give a description of the image features. Another representations to be considered are fractal statistical auto-similar transformation. It has shown that can generate close representations of images, especially in

TABLE I  
ESTIMATED VALUES OF  $\mathbf{H}_h$  FOR A CONSIDERED SET OF *Art* DATABASE

	$\mathbf{H}_1(\mathbf{X})$	$\mathbf{H}_1(\mathbf{T}_\psi\mathbf{X})$			$\mathbf{H}_2(\mathbf{T}_\psi\mathbf{X})$			$\mathbf{H}_3(\mathbf{T}_\psi\mathbf{X})$		
		$j=3$	$j=4$	$j=5$	$j=3$	$j=4$	$j=5$	$j=3$	$j=4$	$j=5$
V-bars	1.0	1.36	1.16	0.98	0.43	0.48	0.48	0.15	0.15	0.14
Centered squares	0.81	0.17	0.14	0.11	0.14	0.14	0.12	0.05	0.05	0.04
Chessboard	1.0	1.67	1.41	1.01	0.81	0.79	0.69	0.33	0.33	0.32
H-bars	1.0	1.36	1.16	0.98	0.41	0.46	0.45	0.32	0.32	0.32
Small squares	0.54	1.2021	1.01	0.82	0.78	0.71	0.65	0.38	0.34	0.34

TABLE II  
 $\mathbf{H}_h$  FOR SET *Nat*

	$\mathbf{H}_1(\mathbf{X})$	$\mathbf{H}_1(\mathbf{T}_\psi\mathbf{X})$			$\mathbf{H}_2(\mathbf{T}_\psi\mathbf{X})$			$\mathbf{H}_3(\mathbf{T}_\psi\mathbf{X})$		
		$j=3$	$j=4$	$j=5$	$j=3$	$j=4$	$j=5$	$j=3$	$j=4$	$j=5$
Bikes	7.35	2.77	2.15	1.69	0.77	0.91	0.98	0.15	0.22	0.32
House	7.18	2.04	1.53	0.96	0.93	0.99	0.87	0.33	0.39	0.48
Plane	6.33	1.78	0.94	0.51	1.02	0.82	0.54	0.36	0.39	0.28
Womanhat	7.11	1.79	1.34	0.68	0.96	0.97	0.66	0.39	0.44	0.35
Mean value	7.33	2.32	1.61	1.14	0.88	0.91	0.84	0.27	0.36	0.38
Std. dev. value	0.34	0.49	0.48	0.40	0.11	0.09	0.15	0.09	0.07	0.07

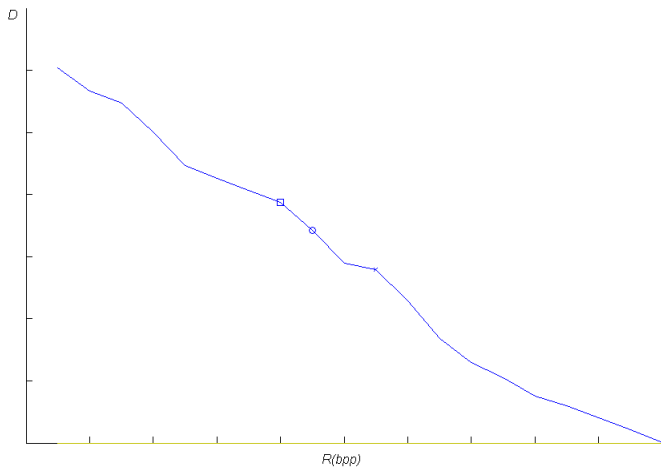


Fig. 8. Rate Distortion curve for the image *ROI-Mammogram*, with the  $\tau(h)$  values. Circle: Distortion calculated at  $\tau(1)$  as detailed in Figure 6(c). Cross: Distortion calculated at  $\tau(2)$  as detailed in Figure 6(d). Square: distortion calculated at  $\tau(3)$ .

order to find tumor growing and organ textures [15]. In another case, Artificial Neural Networks are used to define relevant coefficients used for a selected data base, e.g., lungs in Thorax radiography, breast contour in mammogram [16]. Techniques used to topological dissimilarities, based on a standard-defined structure, are also developed.

## V. CONCLUSIONS

An entropy measure based in Wavelet transform is proposed to provide a shorter search in the Rate-Distortion optimization for image coding. This measure has the property that makes clear the neighbor occurrences, giving information of the relevance of the features that use the redundancy properties of signal. Because the features are described by multi-resolution indexes, some features can be defined by strict information

of components, e.g., entropy of edges can be calculated by using Wavelet detail coefficients from orientation indexes. For instance, this measure is restricted for coding schemes based on Wavelet Transform. However, because the entropy measure involves reduction of spaces, another representations like PCA or Fractal can be considered for specific applications that need a measure of informativity as property of the representation.

Obtained experimental results show that the order of the entropy  $h$  measures the level of spectral dependency of the coefficients. Thus, in order to find a higher dependency order, a scheme for  $h > 3$  can be implemented. However, as  $h$  grows, a higher number of decomposition levels is required, growing its complexity. Finally, the Rate-Distortion optimization initial step can be found by the calculation of  $\mathbf{H}_h(\mathbf{T}_\psi\mathbf{X})$ .

As future work, the estimation of the gradient by information-based entropy remains an open issue. This measure could be used by directional Wavelet families, like *Wedgetlets* or *Contourlets* [17], in order to state a directional information for the information stored in Wavelet coefficients, and to find the approximation of the functional  $g \in W^{k,2}$  in Sobolev spaces. Another work contemplates the use of a statistical information metric to estimate the most-correlated region that can be accessed, by using the Slepian-Wolf Coding [18], and the use of representation set for finding the closest filter that suits for the image region and its neighbors, by using perceptual metrics and information criteria.

## REFERENCES

- [1] D. Taubman, "High performance scalable image compression with ecobit," *IEEE Transactions On Image Processing.*, vol. 9, no. 7, pp. 1158–1170, 2000.
- [2] C.-I. Chang, Y. Du, J. Wang, S.-M. Guo, and P.D. Thouin, "Survey and comparative analysis of entropy and relative entropy thresholding techniques," in *IEE Proceedings Vision, Image and Signal Processing*. IEEE, 2006, pp. 837–850.
- [3] S.-M. Lei and K.-H. Tzou, "Design of high-order conditional entropy coding for images," in *International Conference on Acoustics, Speech, and Signal Processing ICASSP*, I. C. Society, Ed., vol. 3, IEEE. IEEE Press, Marz 1992, pp. 473–476.

- [4] Yun Gao, Ioannis Kontoyiannis, and Elie Bienestock, "Estimating the entropy of binary time series: Methodology, some theory and a simulation study," *Entropy*, no. 10, pp. 71–99, 2008.
- [5] H. Führ, L. Demaret, and F. Friedric, *Document and Image Compression*. CRC Press, 2006, ch. Beyond wavelets: New image representation paradigms.
- [6] P. A. C. Bovik. (2009) Laboratory for image & video engineering. [Online]. Available: <http://live.ece.utexas.edu/>
- [7] H. R. Sheikh, M. F. Sabir, and A. C. Bovik., "A statistical evaluation of recent full reference image quality assessment algorithms." *IEEE Transactions on Image Processing*, vol. 15, no. 11, pp. 3441–3452, 2006.
- [8] J.-C. Garcia-Alvarez, C.-G. Castellanos.Dominguez, and B. Ortiz-Jaramillo, "Image information access using wedgelet filters." IEEE First International Symposium on Applied Sciences in Biomedical and Communication Technologies, October 2008.
- [9] G. Ginesu, F. Massida, and D. Giusto, "A multi-factors approach for image quality assessment based on a human visual system model." *Elsevier Signal Processing: Image Communication.*, no. 21, pp. 316–333, 2006.
- [10] J. Suckling, J. Parker, D. Dance, S. Astley, I. Hutt, C. Boggis, I. Ricketts, E. Stamatakis, N. Cerneaz, S. Kok, P. Taylor, D. Betal, and J. Savage., "The mammographic image analysis society digital mammogram database," *Excerpta Medica, International Congress Series.*, vol. 1069. Database available at <http://peipa.essex.ac.uk/info/mias.html>, pp. 375–378, 1994.
- [11] David Taubman and Robert Prandolini, "Architecture, philosophy and performance of jpeg: Internet protocol standard for jpeg2000," vol. 5150. SPIE International Symposium on Visual Communications and Image Processing VCIP2003, July 2003, pp. 649–663.
- [12] F. A. Llinás, "Model-based jpeg2000 rate control methods." Ph.D. dissertation, Universitat Autònoma de Barcelona, Barcelona, Spain, August 2006.
- [13] O. Kosheleva, "On the optimal choice of quality metric in image compression: a soft computing approach," *Soft Comput.*, vol. 8, no. 4, pp. 268–273, 2004.
- [14] Julio Garcia and Germán Castellanos, "Information quantity measure mapped in wavelet space." Fourth International Conference on BroadBand Communications, Information Technology and Biomedical Applications, Wroclaw, Poland.
- [15] C. Cabrelli, "Fractal block-coding: A functional approach for image and signal processing." *Elsevier Computers and Mathematics with Applications.*, no. 44, pp. 1183–1200, 2002.
- [16] L. F. Pulido, "Recuperación de imágenes combinando redes neuronales y wavelets," Master's thesis, Instituto Naciona de Astrofísica, Óptica y Electrónica, Mexico, 2001.
- [17] L. Demaret, F. Friedrich, H. Führ, and T. Szygowski, "Multiscale wedgelet denoising algorithms." SPIE 5914, 59140x, 2005.
- [18] Ngai-Man Cheung, Caimu Tang, Antonio Ortega, and Cauligi S. Raghavendra., "Efficient wavelet-based predictive slepian-wolf coding for hyperspectral imagery." *Elsevier Journal of Signal Processing.*, no. 86, pp. 3180–3195, 2006.